Luminescence based measurements in micro cavitating flow

D. Podbevšek[1], D. Colombet[2], F. Ayela[2], H. T. T. Lai[1], M. Martini[1], O. Tillement[1], G. Ledoux[1,*]

[1]*Institut Lumière Matière, Université Claude Bernard Lyon 1, 69622 Villeurbanne, France.*

[2]*Laboratoire des Écoulements Géophysiques et Industriels, Domaine Universitaire, 38400 Saint Martin d'Hères, France.*

Abstract

Microchannels are often used to study fluid dynamics. For steady state problems like cavitating flow, fluorescent microscopy, with the addition of temperature sensitive nanoprobes into the observed fluid, can be used to determine the temperature at a chosen point, averaged over the integration time. Coupled with a confocal microscope setup, we are able to produce two and three dimensional temperature maps of the flow in the microchannel by the use of ratiometric intensity measurements. The nanometric scale of the probes assures fast thermalization of the probes and below certain concentrations does not modify the properties of the studied liquid. Since the probes are not present in the vapor phase, the relative intensity map also corresponds to the average void fraction in the flow. These nanoprobes are composed of a gold core and a polysiloxane shell containing fluorescent dyes (FITC, RBITC). Organic dyes were chosen due to their compatibility with the shell and primarily for the fast luminescence lifetime, which is essential due to the rapid flow in the microchannel and the consequent short dwell time of an individual nanoprobe in the excitation volume. The temperature information in each measured point is obtained from the temperature sensitive spectrum of the dye. The shell protects the dye from the environment and allows for the functionalization of the surface to prevent agglomeration, while the gold core mitigates photo bleaching. The technic allowed us to observe temperature gradients in microfluidic two-phase flow and observe the thermal effect associated with phase transition. Typically, a region of decreased temperature is observed downstream the orifice in the liquid-vapor stream, attributed to the cooling of the liquid due to the latent heat of the phase change. However, small changes in the diaphragm geometry can induce recirculating vortices, where the vapor bubbles condensate and induce a region of increased temperature.

Keywords: Cavitation, microchannel, nanoprobes, temperature, thermal effect.

Introduction

Microfluidic devices are frequently used to study fluid dynamics, primarily when specialized liquids are used, which are often hard to synthesize in volume (nanofluids). A narrow opening in a microfluidic channel will accelerate the liquid and, in accordance with Bernoulli's principle, cause the pressure locally to drop. When the pressure decreases below vapor pressure, the liquid will become metastable and eventually vapor bubbles appear. These bubbles grow in the low pressure region and collapse violently upon exiting, which leads to a steady state two-phase flow downstream of the constriction (figure 1a). Due to the latent heat linked to the phase transition, temperature gradients are expected in the region of the growth and collapse of the bubbles [1–4]. Radical production has also been observed with cavitation, linked to the violent bubble collapse [5]. The addition of luminescent species into the liquid allows the use of luminescent based technics to yield the information about the local environment [6].

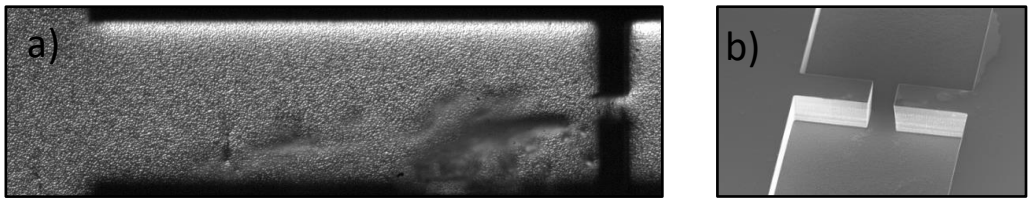

Figure 1: a) Example of cavitating flow in microfluidic channel (8bar driving pressure); flow from right to left. b) SEM image of etched silicon, before sealing the channel with a Pyrex cap. Opening of the constriction in both cases is about 80µm.

The temperature information in each measured point is obtained from the emission spectrum of the dye. On the other hand, with the use of an aqueous solution of luminol as the working fluid, we can probe the radical yield following the violent bubble collapse, via the chemiluminescent pathway. Our aim is to demonstrate the use of luminescent based techniques for sensing in microcavitating flow and show recent developments in the field.

* Corresponding author: gilles.ledoux@univ-lyon1.fr

Body

The use of temperature sensitive luminescent nanoprobes in the observed liquid (water) and the confocal microscope setup for the excitation and detection, makes 2 and 3D characterization of the flow downstream the constriction possible (figure 2). The thermometric method used is called the ratiometric intensity measurement and is the least sensitive to variation in concentration and perturbations due to vapor bubbles in the two-phase flow [1]. It uses the temperature sensitive emission spectra of the fluorophores in the nanoprobe's shell, where the peak shape is altered when the temperature varies. As shown in figure 3b, the ratio of two sections from the normalized emission spectrum corresponds to a given temperature.

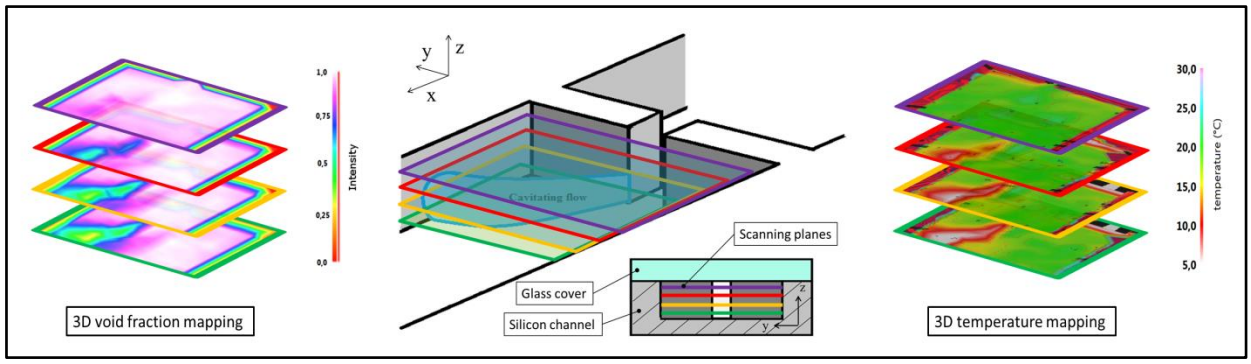

Figure 2: Raster scanning 2d planes at different heights makes 3d characterization of the channels possible. The recorded planes are recorded 20, 50, 70 and 90µm from the transparent wall (cover glass) of the microchannel. The observed two-phase flow and the associated cooling is predominantly located towards the silicon channel wall

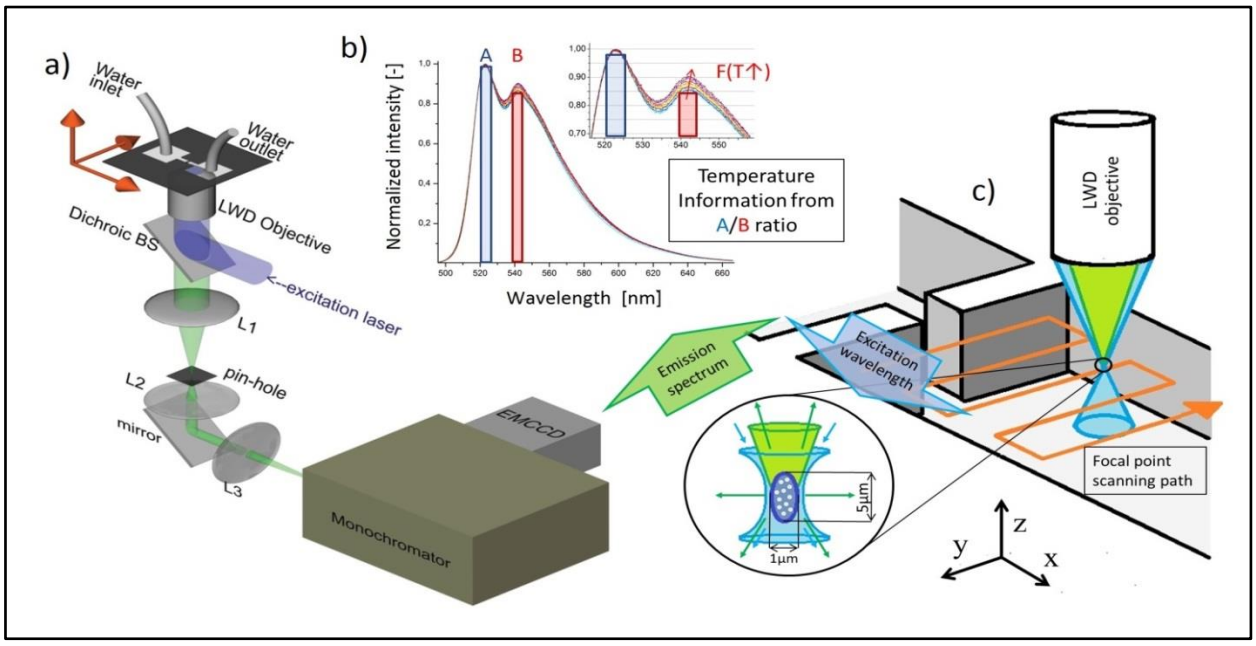

Figure 3: a) confocal microscope detection system, b) emission spectra varying with temperature, ratio of the two peaks yields a value corresponding to a certain temperature, c) focal point raster scanning and emission voxel with excited fluorophores in the nanoprobes producing the emission spectrum.

The encapsulation of the fluorophores into the nanoprobe shell protects them from the hostile environment produced by the violent bubble collapses. Organic dyes were chosen due to their compatibility with the shell and primarily for the fast luminescence lifetime (ns range), which is essential due to the rapid flow in the microchannel (20 – 30 m/s) and the consequent short dwell time of an individual nanoprobe in the excitation volume. The polysiloxane shell protects the dye and also allows for the functionalization of the surface to prevent agglomeration, while the gold core mitigates quenching [7]. The nanometric scale (diameter of 60nm) of the probes assures fast thermalization of

the probes and below certain concentrations does not modify the properties of the studied liquid [8]. The channels used are made by DRIE process on a silicon wafer and anodic bonding of a Pyrex top, described in detail in [8]. These kind of channels have been used extensively by our team [8–10] and others [11–14]. Channel geometries most used are micro diaphragms (figure 1b) and micro Venturis.

The pinhole in the detections system of the confocal microscope is acting as a spatial filter which makes our emission voxel (volume where the signal is collected from) confined in all three directions (Figure 3a,c). By raster scanning an area of interest with this voxel and recording the spectrum in each point, we are able to produce two and three dimensional temperature maps of the flow (figure 2). Furthermore, since the probes are not present in the vapor phase, the relative intensity map also corresponds to the average void fraction in the flow (averaged over the integration time of a single acquisition point).

An example of the recorded temperature gradients and the corresponding intensity map (indication of void fraction) downstream the constriction are show in figure 4 (flow pattern similar to figure 1a). The low temperature region corresponds neatly with the two-phase flow, indicated by lower intensity on the relative intensity map. This indicates that the cooling is most likely linked to the phase transition (latent heat). Using the same technique, an area of heating was identified in a recirculating vortex [1], caused by the bubble collapse (condensation). Although using the same channel design, even slight variations of the channel geometry can cause differences in the resulting flow pattern and produce a stabile recirculating vortex, where bubble collapses are localized.

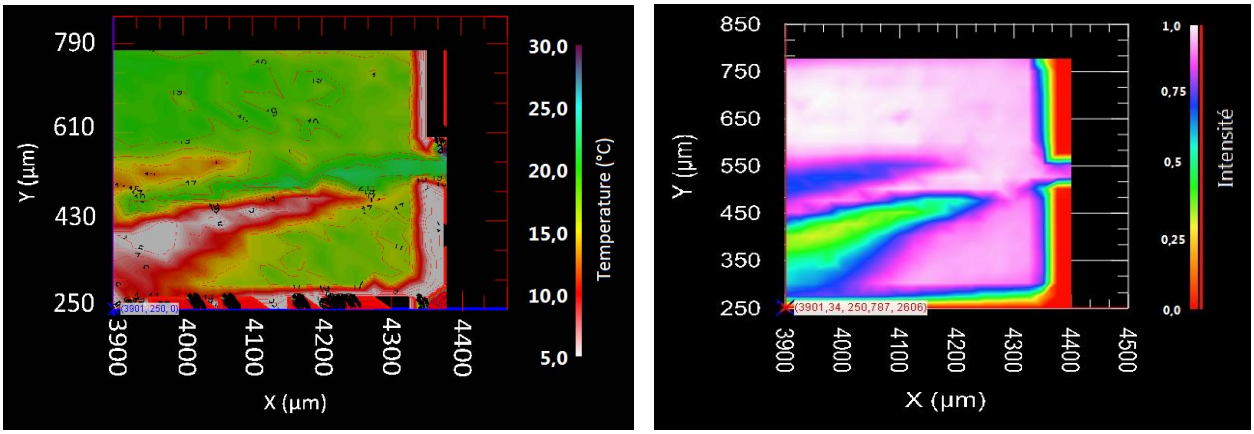

Figure 4: Preliminary temperature and intensity map of flow conditions corresponding to figure 1. Intensity map can be considered the average void fraction mapping, since the dwell time of the vapor phase in the excitation voxel during recording, will yield a proportional drop in intensity. The cooling region and the lower intensity correspond to the two-phase flow region, seen in figure 1. The pressure drop over the microdiaphragm constriction is 10bar, corresponding to flow conditions of about 320µl/s.

A different technique recently developed, allows us to quantify OH radical production in hydrodynamic cavitation. Radical formation has been frequently observed with cavitation and is believed to be linked with the extreme conditions in the bubble implosion. The well-known chemiluminescent reaction of luminol with radical species has been used with ultrasonic cavitation [15–18], while for hydrodynamic cavitation only one previous application was found by the authors [19]. Due to the different bubble dynamics between ultrasonic and hydrodynamic cavitation [20], there were concerns whether there will be significant radical production also for hydrodynamic cavitation [14]. Using an aqueous solution of luminol and the same microfluidic devices as before, the chemiluminescent pathway was used to quantify OH radical production, by a photon counting technique [21]. By placing the photomultiplier tube (PMT) on top of the microfluidic channel, as close as possible to the cavitation active area and using a simple microphone to coordinate when cavitation was occurring, we could observe the well correlated relationship between the cavitation noise and the chemiluminescent signal from the OH/luminol reaction (figure 5). The PMT detects individual photons being produced and by logging the arrival time, the photon yield could be obtained. As the solid detection angle was known and the efficiencies (PMT, quantum yield) estimates in place, we could therefore estimate the actual radical production rate at specific flow conditions. A linear relationship was observed between the flow rate and photon production rate for several microfluidic devices. Considering the relative simplicity of the technique and the ability to quantify radical production, it is a viable option for optimizing radical yield in hydrodynamic flows (biological or chemical wastewater treatment).

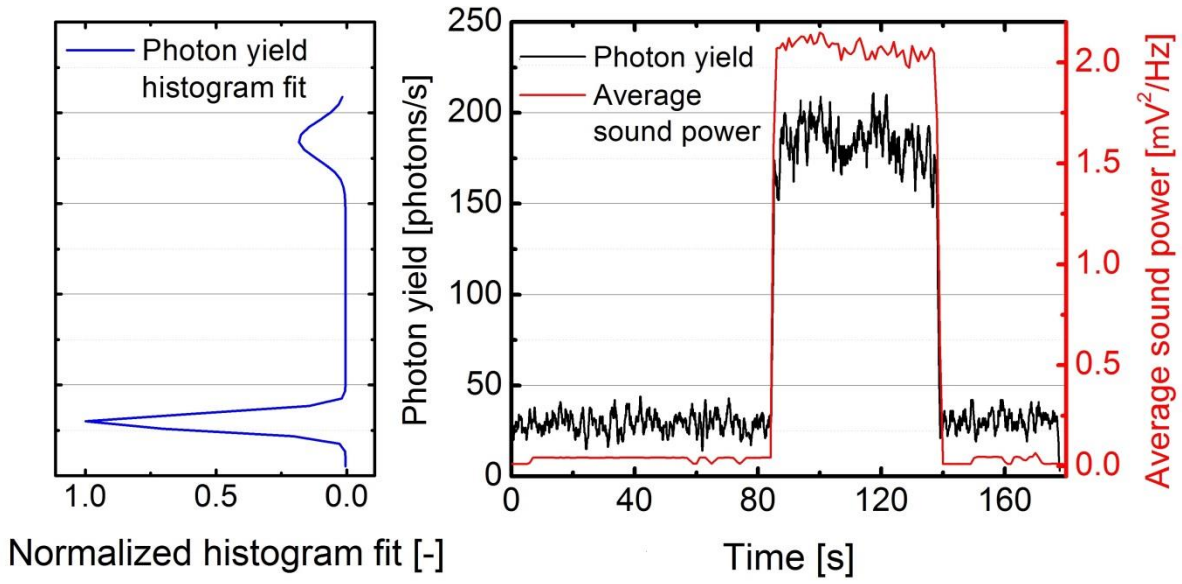

Figure 5: Photon production rate (black) and sound power (red) plotted with time (right) and the fit of the histogram data from the PMT (left). Clearly visible is the correlation between cavitation noise and photon yield. The background signal from the PMT is around 25photons/s which is considered the chemiluminescence off state (no photons being produced). The pressure drop over the microdiaphragm was 10 bar which corresponds to 377µl/s and an average jet velocity of 35.8m/s.

Conclusion

Two luminescence based optical techniques have been demonstrated as a way to probe into the local environment of a microcavitating flow. The temperature dependent emission spectrum of the nanoprobes dispersed in the working liquid, allowed us to observe temperature gradients in microfluidic two-phase flow and the thermal effect associated with phase transition. The preliminary results show a region of decreased temperature observed downstream the orifice in the liquid-vapor stream, as might be expected due to the cooling of the liquid by the phase change transition. The second technique used an aqueous solution of luminol as the working fluid, which allowed the quantification of OH radicals produced by the hydrodynamic cavitation via the chemiluminescent pathway. By using a PMT with photon counting capabilities we could show the correlation of chemiluminescent photon yield to the cavitation noise. As this is a direct and quantitative evidence of OH radical formation in hydrodynamic cavitation, this simple technique could be used for radical production optimization in cavitating flows.

References

[1] Ayela, F., Medrano-Muñoz, M., Amans, D., Dujardin, C., Brichart, T., Martini, M., Tillement, O., and Ledoux, G., 2013, "Experimental Evidence of Temperature Gradients in Cavitating Microflows Seeded with Thermosensitive Nanoprobes," Phys. Rev. E Stat. Nonlin. Soft Matter Phys., **88**(4), p. 043016.
[2] Petkovšek, M., and Dular, M., 2013, "IR Measurements of the Thermodynamic Effects in Cavitating Flow," Int. J. Heat Fluid Flow, **44**(Supplement C), pp. 756–763.
[3] Petkovšek, M., and Dular, M., 2017, "Observing the Thermodynamic Effects in Cavitating Flow by IR Thermography," Exp. Therm. Fluid Sci., **88**(Supplement C), pp. 450–460.
[4] Rimbert, N., Castanet, G., and Funfschilling, D., 2013, "Measurement of Thermal Effects in a Cavitating Channel Flow by 2cLIF."
[5] Arrojo, S., Nerín, C., and Benito, Y., 2007, "Application of Salicylic Acid Dosimetry to Evaluate Hydrodynamic Cavitation as an Advanced Oxidation Process," Ultrason. Sonochem., **14**(3), pp. 343–349.
[6] Valeur, P. D. B., and Berberan-Santos, P. M. N., *Molecular Fluorescence: Principles and Applications, Second Edition*.
[7] Martini, M., Perriat, P., Montagna, M., Pansu, R., Julien, C., Tillement, O., and Roux, S., 2009, "How Gold Particles Suppress Concentration Quenching of Fluorophores Encapsulated in Silica Beads," J. Phys. Chem. C, **113**(41), pp. 17669–17677.
[8] Medrano, M., Zermatten, P. J., Pellone, C., Franc, J. P., and Ayela, F., 2011, "Hydrodynamic Cavitation in Microsystems. I. Experiments with Deionized Water and Nanofluids," Phys. Fluids, **23**(12), p. 127103.

[9] Medrano, M., Pellone, C., Zermatten, P. J., and Ayela, F., 2012, "Hydrodynamic Cavitation in Microsystems. II. Simulations and Optical Observations," Phys. Fluids, **24**(4), p. 047101.
[10] Mossaz, S., Colombet, D., and Ayela, F., 2017, "Hydrodynamic Cavitation of Binary Liquid Mixtures in Laminar and Turbulent Flow Regimes," Exp. Therm. Fluid Sci., **80**(Supplement C), pp. 337–347.
[11] Mishra, C., and Peles, Y., 2005, "Flow Visualization of Cavitating Flows through a Rectangular Slot Micro-Orifice Ingrained in a Microchannel," Phys. Fluids, **17**(11), p. 113602.
[12] Mishra, C., and Peles, Y., 2004, "Cavitation in Flow through a Micro-Orifice inside a Silicon Microchannel," Phys. Fluids, **17**(1), p. 013601.
[13] Mishra, C., and Peles, Y., 2006, "An Experimental Investigation of Hydrodynamic Cavitation in Micro-Venturis," Phys. Fluids, **18**(10), p. 103603.
[14] Rooze, J., André, M., Gulik, G.-J. S. van der, Fernández-Rivas, D., Gardeniers, J. G. E., Rebrov, E. V., Schouten, J. C., and Keurentjes, J. T. F., 2012, "Hydrodynamic Cavitation in Micro Channels with Channel Sizes of 100 and 750 Micrometers," Microfluid. Nanofluidics, **12**(1–4), pp. 499–508.
[15] McMurray, H. N., and Wilson, B. P., 1999, "Mechanistic and Spatial Study of Ultrasonically Induced Luminol Chemiluminescence," J. Phys. Chem. A, **103**(20), pp. 3955–3962.
[16] Hatanaka, S.-I., Mitome, H., Yasui, K., and Hayashi, S., 2002, "Single-Bubble Sonochemiluminescence in Aqueous Luminol Solutions," J. Am. Chem. Soc., **124**(35), pp. 10250–10251.
[17] Price, G. J., Harris, N. K., and Stewart, A. J., 2010, "Direct Observation of Cavitation Fields at 23 and 515kHz," Ultrason. Sonochem., **17**(1), pp. 30–33.
[18] Cao, H., Wan, M., Qiao, Y., Zhang, S., and Li, R., 2012, "Spatial Distribution of Sonoluminescence and Sonochemiluminescence Generated by Cavitation Bubbles in 1.2MHz Focused Ultrasound Field," Ultrason. Sonochem., **19**(2), pp. 257–263.
[19] Schlender, M., Minke, K., and Schuchmann, H. P., 2016, "Sono-Chemiluminescence (SCL) in a High-Pressure Double Stage Homogenization Processes," Chem. Eng. Sci., **142**(Supplement C), pp. 1–11.
[20] Ashokkumar, M., 2011, "The Characterization of Acoustic Cavitation Bubbles – An Overview," Ultrason. Sonochem., **18**(4), pp. 864–872.
[21] Podbevsek, D., Colombet, D., Ledoux, G., and Ayela, F., "Observation of Chemiluminescence Induced by Hydrodynamic Cavitation in Microchannels.," Ultrason. Sonochem. (In Press, Accepted Manuscript - doi:10.1016/j.ultsonch.2018.01.004).